On the Performance of MIMO OFDM-Based Intra-Vehicular VLC Networks

Bugra Turan[1], Omer Narmanlioglu[2], Sinem Coleri Ergen[1] and Murat Uysal[2]

[1]Department of Electrical and Electronics Engineering, Koc University, Sariyer, Istanbul, Turkey, 34450
E-mail: bturan14@ku.edu.tr, sergen@ku.edu.tr
[2]Department of Electrical and Electronics Engineering, Ozyegin University, Istanbul, Turkey, 34794
E-mail: omer.narmanlioglu@ozyegin.edu.tr, murat.uysal@ozyegin.edu.tr

***Abstract*—Vehicular hotspots for on-board Internet access using Long Term Evolution (LTE) as the backhaul network has recently gained popularity. Currently, Wi-Fi is the most common technology to provide in-vehicle access, where data has been relayed through on board LTE receiver. Despite its wide acceptance, coexistence and contention based data rate limitations with Wi-Fi necessitates alternatives for in-vehicle data access schemes. This paper investigates the performance of hybrid LTE and visible light communication (VLC) networks using LTE as the backhaul and VLC as the on-board access network. Under the consideration of vehicle interior unique channel characteristics and light emitting diode (LED) deployment flexibility, best transmitter configuration using repetition coding (RC) and spatial multiplexing (SM) multiple input multiple output (MIMO) modes is determined. Proposed configurations based on direct current biased optical orthogonal frequency-division multiplexing (DCO-OFDM) are compared with respect to their bit-error-rate (BER) performances. Furthermore, the performance of intra-vehicular VLC networks for single and multi-user scenarios is investigated.**

***Index Terms*—Vehicular VLC, optical MIMO, OFDM**

I. Introduction

Vehicles are the third most time spent places, following homes and offices. Hence, in-car Internet access schemes, supporting information and entertainment services such as cloud access, media streaming, content sharing, video conferencing, web browsing are increasingly becoming common. On the other hand, increasing number of connected devices inside the vehicle with the ever increasing high speed connectivity demand requires more bandwidth in addition to radio frequency (RF) coexistence management considerations. As high speed Internet access is key for applications such as smooth media streaming, office and home integration, various RF based technologies have been investigated for intra-vehicular device connectivity [1].

LTE is one of the promising technologies to fulfill quality-of-service (QoS) requirements for in-vehicle connectivity applications. Built-in LTE hot spots with multiple device accesses aim to provide convenience as vehicle on-board LTE receiver is optimized for Doppler shifts and signal fluctuations caused by moving vehicle, in addition to lower device energy needs for connectivity [2]. LTE/Wi-Fi dual-hop architecture is one of the strong candidates to support in-vehicle infotainment applications. However, to take full advantage of LTE data rates with this scheme, wide Wi-Fi channels, susceptible to RF interference and congestion are utilized. Additionally, LTE/Wi-Fi hot spots require additional energy, which may be unfavorable for battery electric vehicles.

As a complementary technology to RF based solutions, VLC is envisaged to be a promising candidate for interference free, high speed intra-vehicular connectivity. Additionally, energy efficiency characteristics of VLC, taking into account limited battery capacity of the electric vehicles and health concerns associated with RF based wireless communications paves a new intra-vehicular wireless communications scheme using intensity modulation and direct detection (IM/DD) of readily available LEDs. It has already been shown that Gbit/s data rates are possible using commercially available white phosphor coated LEDs [3] for indoor VLC.

Optical MIMO techniques [4]–[7] and multicarrier modulation schemes such as OFDM have been studied to achieve high data rates using white LEDs with limited modulation bandwidths. Optical MIMO is also proposed to replace physical transmitter-receiver alignment requirements for line-of-sight (LoS) VLC by electronic alignment [8]. Additionally, various OFDM based schemes are investigated in [9], to inspect possibilities of VLC inside an aircraft cabin. Almost all of the studies considered data communication as a subordinate task to illumination in VLC. However, none of the above works consider MIMO OFDM-based VLC schemes for intra vehicular communications where ambiance lighting with dimmed LEDs in asymmetrical configuration, can be regarded as secondary task to communication.

This paper investigates dual-hop vehicular network based on the usage of LTE as the backhaul and VLC as the in-vehicle access network. LTE provides high speed connectivity optimized at high vehicle mobilities while VLC alleviates in-vehicle wireless coexistence problem. We analyze multiple asymmetrically deployed transmitter LEDs at the vehicle's headliner, serving either single or multiple users, with limited artificial lighting inside the vehicle. The novel contributions of this paper are threefold. First, we select the best LED pair configuration for RC and SM MIMO schemes considering the vehicle interior channel characteristics. Second, employing best LED configuration, we compare the performances of RC and SM modes with different modulation orders. Third, we

determine maximum number of users that can be supported with space-division multiple access (SDMA), considering the proposed LED and photodetector (PD) locations.

The rest of this paper is organized as follows. Section II describes the considered intra-vehicular hybrid LTE/VLC system setup, including DCO-OFDM with optical MIMO techniques. Section III presents utilized channel models. Section IV evaluates the BER performance of the considered system structure. Finally, we conclude the paper in Section V.

Notation: $||.||^2$, $(.)^*$ and $[.]^{\mathrm{T}}$ denote Euclidean distance, complex conjugate and transpose, respectively. $Q(.)$ is the tail probability of standard normal distribution.

II. System Model

Our system structure is depicted in Fig. 1. A vehicle with one or more users driven in a macrocell is considered for downlink transmission. The transmission is modelled as dual-hop including a relay, LTE and VLC links. Relay terminal acts as a backhaul access point for users inside the vehicle.

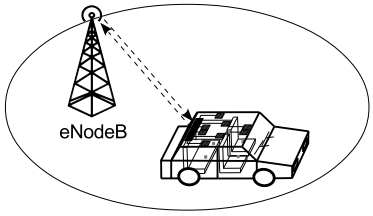

Figure 1: Considered system structure.

Fig. 2 depicts the block diagram of the transmission. The data is transmitted from evolved Node-B (eNodeB) to LTE/VLC relay through the LTE link. Decode-and-forward (DF) relaying procedures are performed such that the data streams are forwarded to each user through VLC links following the decoding and switching processes in the terminal. The uplink transmissions is outside the scope of this work.

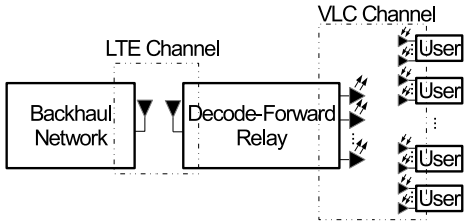

Figure 2: Block diagram of system model.

A. LTE Transmission Model

Orthogonal frequency-division multiple access (OFDMA) is integrated into the physical layer of LTE architecture. In OFDMA, the users are served by using both frequency division multiple access (FDMA) and time division multiple access (TDMA) technologies in which resource blocks (RBs) are a set of 12 subcarriers, each has 15 kHz bandwidth, and allocated to users in each transmission time interval (TTI). With cyclic prefix (CP) appending, linear convolution is turned to circular convolution, where the symbols transmitted through different subcarriers do not interfere with each other as long as the length of CP is equal to or longer than delay spreads of the channel. Furthermore, channel effects can be compensated with simple one tap equalizer.

In OFDMA transmission, first the bit streams are mapped with respect to deployed modulation schemes such as phase-shift keying (PSK) or quadrature amplitude modulation (QAM), then the symbols (X_S) are re-arranged according to resource allocation mechanism and passed through the inverse fast Fourier transform (IFFT). After CP appending, parallel to serial conversion and pulse shaping processes, orthogonal frequency-division multiplexing (OFDM) signals are transmitted through the LTE channel. At the receiver side of relay, assuming no interference from neighbor eNodeBs exist, frequency-domain received signal can be written as,

$$Y_{LTE}[k] = \sqrt{P_{LTE}} X_S[k] H_{LTE}[k] + V_{LTE}[k] \quad (1)$$

where P_{LTE} is the transmit power level of eNodeB, $H_{LTE}[k]$ is the LTE channel frequency response and $V_{LTE}[k]$ is the noise term on k^{th} subcarrier.

In DF relay terminal, the received signals can be optimally decided by *Maximum Likelihood* (ML) decision rule which is expressed by,

$$\hat{X}_S[k] = \underset{X \in \Psi}{\arg\min} \left[\left\| Y_{LTE}[k] - \sqrt{P_{LTE}} H_{LTE}[k] X \right\|^2 \right] \quad (2)$$

where Ψ denotes the constellation points in LTE link.

B. VLC Transmission Model

The decided bits are re-modulated using DCO-OFDM [10] in which Hermitian symmetry and DC bias addition are used to drive the LEDs by real valued and non-negative signals that are the main constraints of IM/DD. When the OFDM frame size without CP is set to N, decided symbols (s), are re-arranged with respect to Hermitian symmetry such as,

$$\mathbf{X}_{VLC} = [0 \; s_1 \; s_2 \; s_3 \; ... \; s_{N/2-1} \; 0 \; s^*_{N/2-1} \; ... \; s^*_2 \; s^*_1]^{\mathrm{T}}, \quad (3)$$

before IFFT process, hence, the output becomes real valued. After CP appending with the length of N_{CP}, a DC bias (V_{bias}) is added to shift the signal into the operation range of the LEDs, limited by turn-on voltage (V_{tov}) and maximum-allowed voltage (V_{max}). Signals beyond this range will be clipped, therefore, we set the signal power level considering the operation range of LEDs.

We consider MIMO system with N_T LEDs and N_R PDs for each user. The frequency-domain received signal on the n^{th} PD can be written as

$$Y_{VLC_n}[k] = \sum_{m=1}^{N_T} \sqrt{\frac{P_{VLC}}{N_T}} R X_{VLC_m}[k] H_{VLC_{nm}}[k] + I_n[k] + V_{VLC_n}[k] \quad (4)$$

where P_{VLC} is total electrical OFDM signal power, R is the optical-to-electrical conversion coefficient (A/W) of PD,

$H_{VLC_{nm}}[k]$ is the frequency response of visible light channel between n^{th} PD and m^{th} LED, $V_{VLC_n}[k]$ is additive white Gaussian noise (AWGN) with zero mean and σ_N^2 variance calculated by N_0W where N_0 is power spectral density and W is system bandwidth at n^{th} PD and $I_n[k]$ is interference from other LEDs on k^{th} subcarrier, written as

$$I_n[k] = \sum_{i=1}^{T} \sum_{m=1}^{N_{T_i}} \sqrt{\frac{P_{VLC}}{N_{T_i}}} R \breve{X}^i_{VLC_m}[k] \breve{H}^i_{VLC_{nm}}[k] \quad (5)$$

where T is the number of active transmission except the considered transmission, N_{T_i} is the number of LEDs used in i^{th} transmission, $\breve{X}_{VLC}[k]$ is DCO-OFDM information signals of users and $\breve{H}_{VLC}[k]$ denotes the interference channel gain.

In RC, each LED is driven by the same information, resulting intensities to constructively add up at the receiver. DCO-OFDM achieves a spectral efficiency of $(\log_2 M)/2$ bit/s/Hz (assume N is large enough) where M is the modulation order. Without any interference, ML decision rule can be written as,

$$\hat{X}_{VLC}[k] = \underset{X \in \Omega}{\operatorname{argmin}} \left(\sum_{n=1}^{N_R} \left\| \frac{Y_{VLC_n}[k]}{\sqrt{\frac{P_{VLC}}{N_T}} R} - X \sum_{m=1}^{N_T} H_{VLC_{nm}}[k] \right\|^2 \right) \quad (6)$$

where Ω is the set of constellation points of deployed modulation scheme in VLC link and signal-to-noise ratio (SNR) per subcarrier is,

$$\mathrm{SNR}_{VLC}[k] = \frac{\frac{P_{VLC}}{N_T} R^2 \sum_{n=1}^{N_R} \left| \left(\sum_{m=1}^{N_T} H_{VLC_{nm}}[k] \right) \right|^2}{\sigma_N^2}. \quad (7)$$

Moreover, subcarrier-based BER can be calculated by (12) (see the top of the next page) [11].

In SM, each LED is simultaneously driven by different information. The enhanced spectral efficiency for SM with DCO-OFDM is $(\min(N_T, N_R) \log_2 M)/2$ bit/s/Hz. Without any interference, ML decision rule is given by,

$$\hat{\mathbf{X}}_{VLC}[k] = \underset{\mathbf{X} \in \mathbf{\Phi}}{\operatorname{argmin}} \left(\left\| \frac{\mathbf{Y}_{VLC}[k]}{\sqrt{\frac{P_{VLC}}{N_T}} R} - \mathbf{H}_{VLC}[k] \mathbf{X} \right\|^2 \right) \quad (8)$$

where $\mathbf{Y}[k]$ is the received signal vector with the dimension of N_R, $\mathbf{H}_{VLC}[k]$ is N_RxN_T channel matrix on the k^{th} subcarrier and Φ includes all possible combinations of transmitted signal vectors. The upper bound of subcarrier based BER values given by ML decision rule can be calculated by (13) (see the top of the next page) where $\mathrm{d_H}(\mathbf{b_{m_1}}, \mathbf{b_{m_2}})$ is Hamming distance of two bit assignments, which are $\mathbf{b_{m_1}}$ and $\mathbf{b_{m_2}}$, of the signal vectors $\mathbf{s_{m_1}}$ and $\mathbf{s_{m_2}}$ [5].

III. Channel Models

A. LTE Channel Model

For urban and suburban areas in macrocell, with the carrier frequency (f_c) of 2 GHz, the channel gain between user equipment (UE) and eNodeB depending on path loss and shadowing effects can be calculated by

$$H = 128 + 37.6 \log(d) + \psi \quad [\mathrm{dB}], \quad (9)$$

where d is the distance between UE and eNodeB in km and ψ (in dB) is log-normal distributed shadowing effect. Additionally, statistical complex-Gaussian multi-path channel model is,

$$h(t) = \sum_{i=0}^{M_t - 1} \alpha_i(t) e^{-j(2\pi f_c \tau_i(t) - \phi_D)} \delta(t - \tau_n(t)) \quad (10)$$

where $\alpha_i(t)$ is the amplitude over i^{th} path at time t, $\tau_n(t)$ is the delay of corresponding path, ϕ_D is denoted by Doppler phase shift and M_t is the total number of resolvable multi-path in a given time interval.

B. VLC Channel Model

The location of LEDs and PDs are shown in Fig. 3. When we consider the base midpoint of the roof as the center, coordinates of the LEDs and PDs are presented in Table I. LEDs are deployed asymmetrically to generate diverse LoS links with different channel gains. Perfect synchronization without time dispersion is assumed for all links with regards to negligible path difference between different transmitter-receiver links.

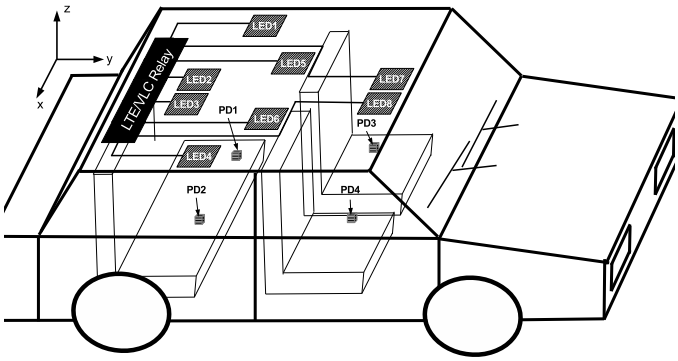

Figure 3: Considered vehicle with LEDs and PDs.

The LoS characteristic of VLC channel is given by,

$$h_{VLC} = \begin{cases} \frac{u+1}{2\pi d_x^2} \cos^u(\phi) \cos(\psi) & 0 \le \psi \le \Psi_{\frac{1}{2}} \\ 0 & \psi \ge \Psi_{\frac{1}{2}} \end{cases} \quad (11)$$

where ϕ is the irradiance angle with respect to LED axis, ψ is the angle of incidence with respect to PD axis, d_x is the distance between LED and PD, $u = -\ln(2) \Big/ \ln\left(\cos\left(\Phi_{\frac{1}{2}}\right)\right)$ where the LED semiangle $\Phi_{\frac{1}{2}}$ is set to $60°$, the field-of-view semiangle of the PD $\Psi_{\frac{1}{2}}$ is assumed to be $60°$.

Table I: Coordinates of LEDs and PDs

LED 1	(-0.35,-0.60,1.20)		**PD 1a**	(-0.45,-0.50,0.50)
LED 2	(-0.70,-0.20,1.20)		**PD 1b**	(-0.45,-0.30,0.50)
LED 3	(-0.70,+0.20,1.20)		**PD 2a**	(-0.45,+0.30,0.50)
LED 4	(-0.35,+0.60,1.20)		**PD 2b**	(-0.45,+0.50,0.50)
LED 5	(-0.19,-0.40,1.20)		**PD 3a**	(-0.30,-0.50,0.50)
LED 6	(-0.19,+0.40,1.20)		**PD 3b**	(-0.30,-0.30,0.50)
LED 7	(-0.50,-0.30,1.20)		**PD 4a**	(-0.30,+0.30,0.50)
LED 8	(-0.50,+0.30,1.20)		**PD 4b**	(-0.30,+0.50,0.50)

$$\mathrm{BER_{RC}}[k] \approx \left\{ \begin{array}{cc} Q\left(\sqrt{2\mathrm{SNR}[k]}\right) & , \quad 2-\mathrm{PSK} \\ \frac{2\left(\sqrt{M}-1\right)}{\sqrt{M}\log_2\sqrt{M}} Q\left(\sqrt{\frac{3\mathrm{SNR}[k]}{(M-1)}}\right) & , \quad \mathrm{square}-M-\mathrm{QAM} \\ \frac{2}{\log_2(U\mathrm{x}J)}\left[\frac{U-1}{U} Q\left(\sqrt{\frac{6\mathrm{SNR}[k]}{U^2+J^2-2}}\right) + \frac{J-1}{J} Q\left(\sqrt{\frac{6\mathrm{SNR}[k]}{U^2+J^2-2}}\right)\right] & , \quad \mathrm{rectangular}-M=U\mathrm{x}J-\mathrm{QAM} \end{array} \right\} \quad (12)$$

$$\mathrm{BER_{SM}}[k] \leq \frac{1}{M^{N_T}\log_2\left(M^{N_T}\right)} \sum_{m_1=1}^{M^{N_T}} \left(\sum_{m_2=1}^{M^{N_T}} \mathrm{d_H}\left(\mathbf{b_{m_1}}, \mathbf{b_{m_2}}\right) Q\left(\sqrt{\frac{P_{VLC}R^2}{2\sigma_N^2 N_T}\left\|\mathbf{H}[k]\left(\mathbf{s_{m_1}}-\mathbf{s_{m_1}}\right)\right\|^2}\right)\right) \quad (13)$$

IV. Numerical Results

In this section, we present numerical results to evaluate the performance of intra-vehicular VLC network. Simulation parameters are shown in Table II. In all simulations, we assume that perfect channel state information (CSI) is available at the source, relay and destination terminals. In a LTE/VLC dual-hop system including DF relaying, subcarrier-based end-to-end BER can be calculated by

$$\begin{aligned} \mathrm{BER}[k] = &\left(1-\mathrm{BER}_{LTE}[k]\right)\mathrm{BER}_{VLC}[k] \\ &+\mathrm{BER}_{LTE}[k]\left(1-\mathrm{BER}_{VLC}[k]\right). \end{aligned} \quad (14)$$

Relatively, end-to-end BER can be calculated as averaging the subcarrier-based BER values. Even though BER_{LTE} can be calculated using (9) and (10), target packet error rate of 10^{-6} is considered as in Transmission Control Protocol (TCP)-based applications [12] which can be satisfied using additional techniques (i.e., adaptive modulation and coding (AMC) and hybrid automatic repeat request (HARQ)).

Table II: Simulation Parameters.

LED modulation bandwidth (W)	20 MHz
Power spectral density of VLC noise (N_0)	8.1x10^{-19} W/Hz
Responsivity of PD (R)	0.54 A/W
Turn-on voltage (V_{tov})	1.7 V
Maximum allowed voltage (V_{max})	2.2 V
Bias voltage (V_{bias})	1.95 V
Number of subcarrier (N)	64
Length of cyclic prefix (N_{CP})	4

In Fig. 4, we present end-to-end BER performances of RC and SM MIMO modes with respect to different LED transmitter selections while first user's PDs (PD 1a and PD 1b) are selected at the receiver side. Theoretical BER approximation of RC given by (12) and upper bound of SM given by (13) are depicted as solid lines while Monte Carlo simulation results are shown by markers. The results reveal that selection of 1^{st} and 2^{nd} LEDs (see Fig. 4 (a)) gives the best performance in terms of BER for RC since they are the closest points to selected PDs. On the other hand, the lowest BER can be achieved by 1^{st} and 3^{rd} LEDs (see Fig. 4 (b)-(c)) for SM since the channel correlation is another critical factor that affects the performance in addition to path loss. When BER performances are compared with respect to selected modulation order sizes (see Fig. 4 (b)-(c)), the orders of LED transmitter selection differs. This can be explained by the term of $||\mathbf{H}[k]\left(\mathbf{s_{m_1}}-\mathbf{s_{m_1}}\right)||^2$ in (13).

In Fig. 5, we present the BER performance of RC and SM with respect to different spectral efficiencies using best two LEDs selection according first user's PDs. For 1 bit/s/Hz (RC 4-QAM/SM 2-PSK), RC outperforms SM with the gain of 7.44 dB at the target of 10^{-3} BER. However, when we increase the spectral efficiency respectively to 2, 3 and 4 bit/s/Hz, the gain decreases to 3.71 dB, 4.34 dB and 1.07 dB. On the other hand, comparing RC 1024-QAM with SM 32-QAM (5 bit/s/Hz), SM outperforms RC with the gain of 1.64 dB. This amount increases to 4.27 dB for the spectral efficiency of 6 bit/s/Hz. These results reveal that RC is more robust to channel correlation, however, it requires larger modulation order to achieve the same spectral efficiency as SM, thereby, it performs worse at the higher modulation orders.

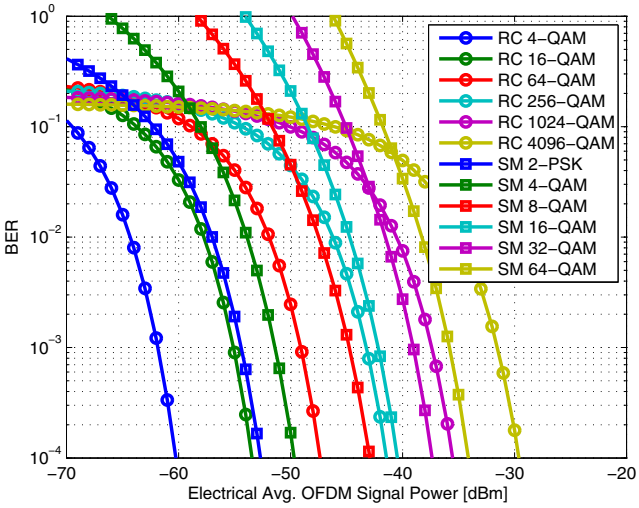

Figure 5: BER performances with different modulation orders.

In Fig. 6, we present the BER performance of single and multi-user scenarios where 4-QAM is set as the modulation order with both 1x1 and 2x2 RC MIMO configurations. The results indicate that multiple users can be served by SDMA up to three users with specific locations due to PD's limited field-of-view. However, when this limit is exceeded, orthogonal multiple access mechanisms such as TDMA, FDMA etc. can

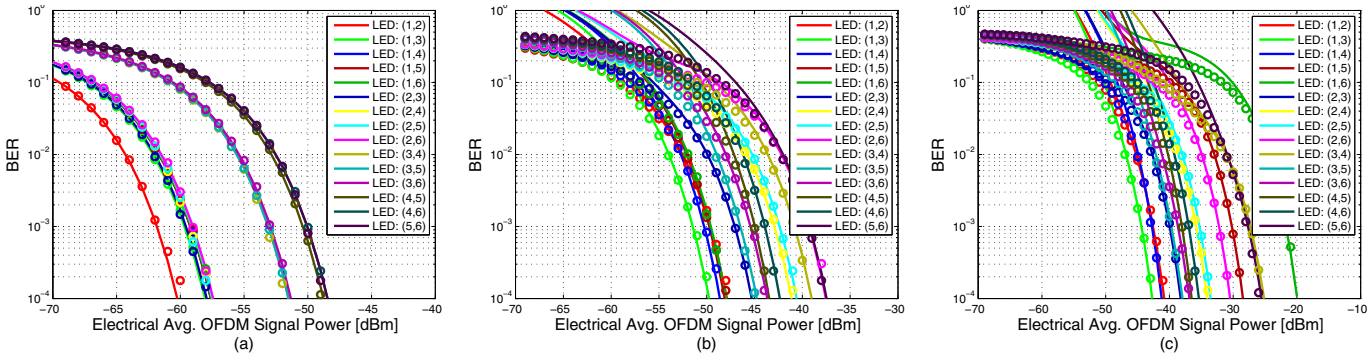

Figure 4: BER performances with different LEDs when (a) RC 4-QAM, SM (b) 4-QAM and (c) 16-QAM are considered.

be employed because of the interference issues. Additionally, transmit and receive diversity improves the performance with the gain of 3.52 dB, 1.51 dB and 2.49 dB for the single, two and three user cases, respectively.

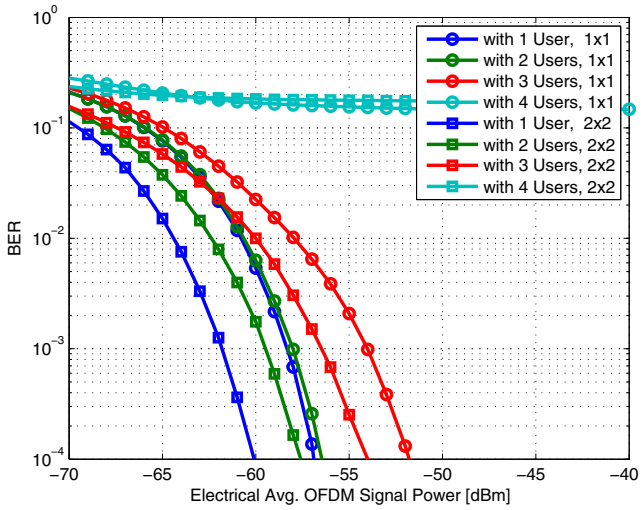

Figure 6: BER performances with different user sizes.

V. Conclusion

In this paper, we addressed the optical transmitter selection and evaluated different optical MIMO schemes with varying modulation orders for LTE/VLC intra-vehicular network. We have shown that under limited transmitter-receiver path length, illumination and direct LoS channel conditions, LED transmitter selection is key to achieve low BER with regards to the selected MIMO scheme. Our simulation results indicate that nearby transmitters are favorable for RC due to high SNR requirement, whereas SM additionally requires low channel correlation. It has also been shown that SM outperforms RC at high spectral efficiencies, as RC requires higher constellation sizes. Finally, it has been demonstrated that proposed transmitter configuration can support up to three users by SDMA.

VI. Acknowledgement

Our work was supported by Argela and Turk Telekom under Grant Number 11315-07. Sinem Coleri Ergen acknowledges support from Bilim Akademisi- The Science Academy, Turkey under the BAGEP program, and the Turkish Academy of Sciences (TUBA) within the Young Scientist Award Program (GEBIP).

References

[1] N. M. Sadek, H. H. Halawa, R. M. Daoud, H. H. Amer, and N. A. Ali, "Heterogeneous lte/wi-fi architecture for its traffic control and infotainment," in *2015 International Conference on Electrical Systems for Aircraft, Railway, Ship Propulsion and Road Vehicles (ESARS)*, pp. 1–6, March 2015.

[2] N. Lu, N. Cheng, N. Zhang, X. Shen, and J. W. Mark, "Connected vehicles: Solutions and challenges," *IEEE Internet of Things Journal*, vol. 1, pp. 289–299, Aug 2014.

[3] L. Zeng, D. C. O'Brien, H. L. Minh, G. E. Faulkner, K. Lee, D. Jung, Y. Oh, and E. T. Won, "High data rate multiple input multiple output (mimo) optical wireless communications using white led lighting," *IEEE Journal on Selected Areas in Communications*, vol. 27, pp. 1654–1662, December 2009.

[4] A. Stavridis and H. Haas, "Performance evaluation of space modulation techniques in vlc systems," in *2015 IEEE International Conference on Communication Workshop (ICCW)*, pp. 1356–1361, June 2015.

[5] T. Fath and H. Haas, "Performance comparison of mimo techniques for optical wireless communications in indoor environments," *Communications, IEEE Transactions on*, vol. 61, no. 2, pp. 733–742, 2013.

[6] Y. Hong, T. Wu, and L. K. Chen, "On the performance of adaptive mimo-ofdm indoor visible light communications," *IEEE Photonics Technology Letters*, vol. 28, pp. 907–910, April 2016.

[7] P. F. Mmbaga, J. Thompson, and H. Haas, "Performance analysis of indoor diffuse vlc mimo channels using angular diversity detectors," *Journal of Lightwave Technology*, vol. 34, pp. 1254–1266, Feb 2016.

[8] L. Zeng, D. C. O'Brien, H. L. Minh, G. E. Faulkner, K. Lee, D. Jung, Y. Oh, and E. T. Won, "High data rate multiple input multiple output (mimo) optical wireless communications using white led lighting," *IEEE Journal on Selected Areas in Communications*, vol. 27, pp. 1654–1662, December 2009.

[9] S. Dimitrov, H. Haas, M. Cappitelli, and M. Olbert, "On the throughput of an ofdm-based cellular optical wireless system for an aircraft cabin," in *Proceedings of the 5th European Conference on Antennas and Propagation (EUCAP)*, pp. 3089–3093, April 2011.

[10] J. Armstrong, "Ofdm for optical communications," *Lightwave Technology, Journal of*, vol. 27, no. 3, pp. 189–204, 2009.

[11] K. Cho and D. Yoon, "On the general ber expression of one-and two-dimensional amplitude modulations," *Communications, IEEE Transactions on*, vol. 50, no. 7, pp. 1074–1080, 2002.

[12] F. Capozzi, G. Piro, L. A. Grieco, G. Boggia, and P. Camarda, "Downlink packet scheduling in lte cellular networks: Key design issues and a survey," *Communications Surveys & Tutorials, IEEE*, vol. 15, no. 2, pp. 678–700, 2013.

[13] S. Wu, H. Wang, and C.-H. Youn, "Visible light communications for 5g wireless networking systems: from fixed to mobile communications," *Network, IEEE*, vol. 28, no. 6, pp. 41–45, 2014.